Automatic Image Detection of Halloysite Clay Nanotubes as a Future Ultrasound Theranostic Agent for Tumoral Cell Targeting and Treatment

Sergio Casciaro, *IEEE Member*, Giulia Soloperto, Francesco Conversano, *IEEE Member*, Ernesto Casciaro, *IEEE Member*, Antonio Greco, Stefano Leporatti, Aimè Lay-Ekuakille, *IEEE Senior Member,* Giuseppe Gigli.

***Abstract*— Halloysite clay Nanotubes (HNTs) are nanomaterials composed of double layered aluminosilicate minerals with a hollow tubular structure in the submicron range. They are characterized by a wide range of applications in anticancer therapy as agent delivery. In this work we aim to investigate the automatic detection features of HNTs through advanced quantitative ultrasound imaging employing different concentrations (3-5 mg/mL) at clinical conventional frequency, i.e. 7 MHz. Different tissue mimicking samples of HNT containing agarose gel were imaged through a commercially available echographic system, that was opportunely combined with ultrasound signal analysis research platform for extracting the raw ultrasound radiofrequency (RF) signals. Acquired data were stored and analyzed by means of an in-house developed algorithm based on wavelet decomposition, in order to identify the specific spectrum contribution of the HNTs and generate corresponding image mapping. Sensitivity and specificity of the HNT detection were quantified. Average specificity (94.36%) was very high with reduced dependency on HNT concentration, while sensitivity showed a proportional increase with concentration with an average of 46.78%. However, automatic detection performances are currently under investigation for further improvement taking into account image enhancement and biocompatibility issues.**

***Index Terms* — molecular imaging, cancer detection, nanoparticles, halloysite nanotubes, tissue typing, biomedical signal processing, theranostics, cell targeting, drug delivery.**

I. Introduction

NEW targeted ultrasound contrast agents (UCA) are playing a key role with the rapid development of contrast-enhanced ultrasound technology, showing good prospects for applications in molecular imaging and targeted therapy [1]. Overcoming all main limitations presented by traditional microbubble UCAs in relationship to their specific intra-vascular applications [2]-[4], novel nanoparticles allow cell targeting beyond capillary vasculature, such as cancer cells [5]-[8] without using expensive and health threatening ionizing techniques such as Positron Emission Tomography (PET), often used in association with MRI or CT [9], with additional radiation dose in this case, for obtaining suitable anatomical information.

Echographic imaging is the most widely available medical imaging modality, owing to its inexpensiveness, safety and real-time features [10]. Nonetheless, healthy and pathologic tissues do not normally present sufficient discriminating scattering of ultrasound waves and UCA image enhancement is necessary to provide optimal contrast and enable tissue typing in ultrasonographic imaging. Additionally, novel cellular drug delivery experimental agents, including halloysite clays nanotubes (HNT), have been successfully tested on cellular and animal models. Specifically, halloysite clay is a two-layered aluminosilicate with a hollow tubular structure (50 to 70 nm in external diameter, 15 nm diameter lumen and 1 ± 0.5 μm length) and chemically similar to kaolin [11-13]. HNT is a natural product made of inexpensive materials [14] with a simple means of fabrication and selective labeling of the inner and outer surfaces. HNTs are therefore capable of entrapping and release active agents within the inner lumen, as successfully tested on various applications on both cellular and animal models [15-18].

In this article, we experimentally investigated and optimized the automatic detection features of HNTs through advanced quantitative ultrasound imaging employing different concentrations (3-5 mg/mL) and a conventional frequency (7 MHz) for future application of tissue typing through functionalized HNTs.

II. Materials and Methods

A. HNT containing Tissue-mimicking Phantom

Purified dehydrated HNTs were obtained from Applied Minerals, Inc. and coated with Methoxy(polyethyleneoxy) propyltrimethoxysilane. To conduct the experiments, HNTs were dispersed in tissue mimicking gel samples, whose employment in the study of signal enhancement produced by solid nanoparticles have been already reported in literature

This work was partially funded by the grant N° DM18604 – DD MIUR 14.5.2005 n.602 of MIUR, by FESR P.O. Apulia Region 2007-2013 – Action 1.2.4 (grant number 3Q5AX31) and by the Progetto Bandiera NANOMAX ENCODER. G. Soloperto, F. Conversano, A. Greco, and E. and S. Casciaro are with the National Research Council, Institute of Clinical Physiology 73100 Lecce, Italy. (E-mail: sergio.casciaro@cnr.it). S. Leporatti is with National Council of Research, Institute of Nanosciences, Lecce, Italy. G. Gigli and A. Lay-Ekuakille are with Department of Innovation Engineering, University of Salento, Lecce, Italy.

978-1-4673-6386-0/14/$31.00 ©2014 IEEE

[19-22]. In our case, the employment of an agarose gel was particularly suited to identify the specific HNT contribution to the backscatter amplitude with respect to the control, i.e. blank gel samples. [9,19,23]

The amount of 0.5 mL of pure agarose gel (0.4 g/100 mL) was poured into a 2-mL Eppendorf tube. Once the agarose was jellified, the desired amount of HNTs was added to more agarose solution in a vial, and the mixture was sonicated for 30 seconds; 1 mL of this suspension was quickly poured into the Eppendorf tube, and then placed in freezer in order to ensure quick jelling and prevent particle settlement; the adopted concentration amounts of HNTs were quantified in mg/mL and corresponded to 3 and 5 mg of HNT in 1 mL of agarose gel contained in the Eppendorf tube. Each sample was finally layered with 0.5 mL of pure agarose as schemed in Fig. 1.a. Three samples were obtained for each examined HNT concentration and were stored in a refrigerator at 4°C prior to experiments.

B. The Experimental Set-up

Ultrasound images and signals were acquired by means of an experimental set-up composed by:

- a clinically-available digital echograph (MyLab XVG, Esaote Spa, Genoa, Italy) equipped with a linear echographic transducer (LA523, Esaote Spa, Genoa, Italy) power of the transmitted signal = 50%, gain = 50, time gain compensation (TGC) = linear 1dB/cm, frequency 7 MHz.
- a research platform for the acquisition of "raw" RF signals digitized at 50MHz, 16 bit (FEMMINA system, ELEN Spa, Florence, Italy) [23], linked to the echograph by means of an optical fiber (1Gb/s) (850 frames were recorded, at 12 frame per second (fps))
- a motorized mechanism of an infusion pump (KDS 100, KD Scientific Inc., Holliston, MA) on which the probe was mounted in order to perform automatic and repeatable scanning of the phantom (constant scansion speed of 12.5 mm/min).
- a distilled water tank with a fixed support for the Eppendorf phantom at the bottom.

The US probe, partially immersed in water, was positioned perpendicular to the sample surface at such a distance that the transducer focus (set to 2 cm) was located half-way through the studied sample depth. Echographic image were composed by raw data acquired with 152 tracks x 2980 points/track. An example of the resulting B-mode image, acquired on the control phantom, is presented in Fig 1.b

C. Data Analysis

Information content only available in the raw RF signals, acquired through FEMMINA [24], was analyzed by means of a software tool for wavelet decomposition and spectral analysis (RULES, ELEN SpA, Florence, Italy [25].

The RF acquired data were then off-line processed to find a specific algorithm configuration to selectively discriminate the HNT-containing layer from the surrounding layers of pure agarose gel and obtain color map, superimposed to B-mode images, in which the HNT were selectively displayed.

The employed mother wavelet was Daubechies16, biorthogonal and symmetric, and discrete wavelet packets transform (DWPT) was realized by means of a parallel architecture of the Mallat algorithm [26].

The final output of this algorithm was the superimposition of a specific color map identifying the presence of HNTs on each of the 300 acquired echographic image frames, selected in correspondence to the central portion of the Eppendorf in order to prevent boundary effects. These sequences were then processed through a custom-developed software tool implemented in MatLab 7.0 (The MathWorks, Natick, MA), for counting the number of colored pixels in each frame, distinguishing in the Region of interest (ROI, as in Fig. 1.b) between "true positives" (TP, ie, pixels actually belonging to the HNT-containing layer) and "false positives" (FP, ie, pixels not belonging to the target layer), so sensitivity and specificity of the detection technique, was calculated as follows [27]:

$$\text{Sensitivity } [\%]=100\text{x}TP/(TP+FN) \quad (1)$$

$$\text{Specificity } [\%]=100\text{x}TN/(TN+FP) \quad (2)$$

where FN denotes the "false negatives" (i.e., pixels belonging to the HTN-containing layer but not identified by the algorithm) and TN are the "true negatives" (i.e., pixels not belonging to the target layer and were not colored by the algorithm). Each parameter was averaged over the 300 frames and over the triplicate samples per concentration. The same RULES configuration was used for both tested HNT concentration and the parameter optimization responded to the following criteria: (1) detection of the HNT containing layer; (2) minimization of the FP appearance outside the HNT-containing layer; (3) minimization of the FN appearance on the control phantom.

III. RESULTS

In these experiments we explored the possibility of exploiting information introduced by the HNTs into the spectrum of the RF signal. We qualitatively demonstrates how a tissue mimicking layer containing HNTs placed between other two

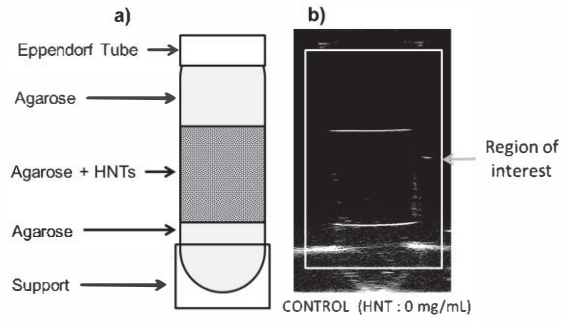

Fig. 1. (a) Scheme of the analyzed phantom; (b) B-mode image of a control phantom with indication of the chosen Region of Interest (ROI).

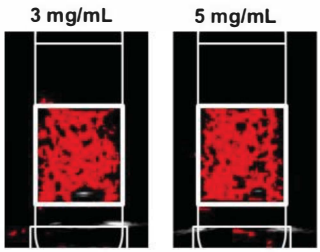

Fig. 2. B-mode image of a control phantom with indication of the HNT-containing layer with automatic detection color maps displayed for 3 and 5 mg/mL, as indicated.

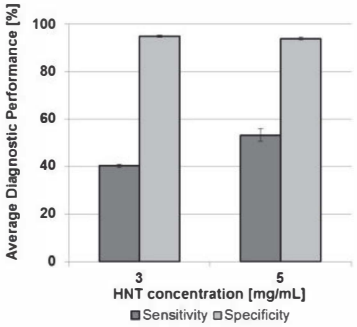

Fig. 3. Performances of the automatic HNT detection algorithm quantified in sensitivity and specificity as function of HNT concentration. Values are calculated over 300 frames corresponding to the central portion of each imaged phantom and averaged over the triplicate samples per concentration. (Error bars represent standard deviations).

layers of the same material in a pure state can be automatically and selectively detected in the corresponding echographic images. Results obtained by applying a specific custom-developed optimized configuration at 7 MHz within the software RULES are qualitatively illustrated in Fig. 2.

To quantitatively evaluate the performances of the adopted methodology, sensitivity and specificity were calculated. Our results denote that sensitivity values increased from the lowest to the highest employed HNT concentration, whereas specificity decreased of a considerably smaller amount (Fig.3). Specifically, average specificity (94.36%) was very high with reduced dependency on HNT concentration, while sensitivity showed a proportional increase with concentration with an average of 46.78%.

IV. Discussions

Feasibility of ultrasound molecular imaging at clinical frequencies employing commercially available echographs and inorganic nanoparticles and nanocomposites have been demonstrated showing their diagnostic suitability as UCAs [19], [28], allowing harmonic ultrasound imaging [29] and multimodal imaging combining ultrasound and magnetic resonance imaging [29]-[31]. Nonetheless, the diagnostic potential of HNT employment in conjunction with echographic imaging techniques is still underexplored [32]. Our in vitro experiments documented the feasibility of enhanced tissue typing through HNTs with conventional echographic systems and represent to date the first evidences of the possibility of such application.

From the qualitative evaluation of the automatic detection performances of our methodology, both employed HNT concentrations appeared to allow satisfactory tissue discrimination. In fact very few areas of FP are identifiable outside the portion of the images occupied by the HNT containing layer. The corresponding quantification of the performances of the automatic detection of HNTs confirmed these findings with satisfactory values of specificity and sensitivity. The present study identified the value of 3 mg/mL as the best of the two tested HNT concentration to be employed for ultrasound targeted imaging purposes. This specific concentration, in fact, offers the opportunity of reducing the HNT dose at the expenses of detection sensitivity but still preserving segmentation accuracy on conventional echographic images, since the HNT characteristic "signature" in the corresponding RF signal is extremely detectable and comparable with the other value of concentration used. Nonetheless further studies are needed to document the biocompatibility profile of HNTs in this dose range and to possibly extend the automatic detection methodology to lower levels of concentration.

V. Conclusions

The automatic detection features of HNTs in conjunction with conventional echographic system have been preliminarily evaluated in this work. The methodology was tested in vitro and resulted feasible for the concentration range 3-5 mg/mL investigated with an ultrasonic frequency of 7 MHz. Both employed concentrations demonstrated satisfactory diagnostic performance, although 3 mg/mL is the value that better compromise with safety issues possibly arising from future employment of this tissue typing technique in vivo. In fact, whereas cellular and animal studies of HNT tolerability are available, future work will be devoted to further characterize HNT as UCA and theranostic vector for clinical application.

References

[1] F. Yang, Z. Y. Chen, and Y. Lin, "Advancement of targeted ultrasound contrast agents and their applications in molecular imaging and targeted therapy," *Curr. Pharm. Des.* 2012 [Epub ahead of print].

[2] S. Unnikrishnan, and A. L. Klibanov, "Microbubbles as ultrasound contrast agents for molecular imaging: preparation and application," *AJR Am. J. Roentgenol.*, vol. 199, no. 2, pp. 292-299, Aug. 2012.

[3] F. Kiessling, S. Fokong, P. Koczera, W. Lederle, and T. Lammers, "Ultrasound microbubbles for molecular diagnosis, therapy, and theranostics," *J. Nucl. Med.*, vol. 53, no. 3, pp. 345-348, Mar. 2012.

[4] J. Liu, A. L. Levine, J. S. Mattoon, M. Yamaguchi, R. J. Lee, X. Pan, and T. J. Rosol, "Nanoparticles as image enhancing agents for ultrasonography," *Phys. Med. Biol.,* vol. 51, no. 9, pp. 2179-2189, May 2006.

[5] S. Casciaro, "Theranostic applications: Non-ionizing cellular and molecular imaging through innovative nanosystems for early diagnosis and therapy," *World J. Radiol.,* vol. 3, no 10, pp. 249-255, Oct. 2011.

[6] G. Pascali, F. Conversano, S. Casciaro, and P. A. Salvadori, "Translational perspectives in molecular imaging: methodological evolution and nanostructured materials," *Recenti Prog. Med.,*vol. 103, no. 4, pp. 142-153, Apr. 2012.

[7] G. Soloperto, and S. Casciaro, "Progress in atherosclerotic plaque imaging," *World J Radiol.,* vol. 4, no. 8, pp. 353-371, Aug. 2012.

[8] F. Conversano, R. Franchini, C. Demitri, L. Massoptier, F. Montagna, A. Maffezzoli, A. Malvasi, and S. Casciaro, "Hepatic vessel segmentation for 3D planning of liver surgery: experimental evaluation of a new fully automatic algorithm," *Acad. Radiol.,*vol. 18, no. 4, pp. 461-470. Apr. 2011.

[9] M. Postema, and O. H. Gilja, "Contrast-enhanced and targeted ultrasound," *World J. Gastroenterol.*, vol. 17, no. 1, pp. 28-41, Jan. 2011

[10] E. Joussein, S. Petit, J. Churchman, B. Theng, D. Righi, and B. Delvaux, "Halloysite Clay minerals: a review," *Clay Minerals,* vol. 40, pp.383-426, 2005

[11] G. Tari, I. Bobos, C. Gomes, and J. Ferreira, "Modification of surface charge properties during kaolinate to halloysite-7A transformation," *J. Colloid. Interface Sci.,*vol. 210, no. 2, pp. 360-369, Feb. 1999.

[12] R. Price, B. Gaber, and Y. Lvov, "Release characteristics of tetracycline, khellin and NAD from halloysite: a cylindrical mineral for delivery of biologically active agents," *J. Microencapsulation,* vol. 18, no. 6, pp.713–722, Nov. 2001

[13] V. Vergaro, Y. M. Lvov, and S. Leporatti, "Halloysite clay nanotubes for resveratrol delivery to cancer cells," *Macromol. Biosci.*, vol. 12, no. 9, pp. 1265-1271, Sep. 2012.

[14] E. Abdullayev, R. Price, D. Shchukin, and Y. Lvov, "Halloysite tubes as nanocontainers for anticorrosion coating with benzotriazole," *ACS Appl. Mater. Interfaces.*, vol. 2, no. 7, pp. 1437-1443, Jul. 2009.

[15] N. Veerabadran, D. Mongayt, V. Torchilin, R. Price, and Y. Lvov, "Organized shells on clay nanotubes for controlled release of macromolecules," *Macromol. Rapid. Commun.*, vol. 30, no. 2, pp. 94-99. Jan. 2009.

[16] D. Kommireddy, I. Ichinose, Y. Lvov, and D. Mills, "Nanoparticle multilayer: surface modification for cell attachment and growth," *J. Biomed. Nanotechnol.*, vol. 1, no. 4, pp. 286-290, Dec. 2005

[17] H. Kelly, P. Deasy, E. Ziaka, and N. Claffey, "Formulation and preliminary in vivo dog studies of a novel drug delivery system for the treatment of periodontitis," *Int. J Pharm.*, vol. 274, no 1-2, pp. 167-183, Apr. 2004.

[18] S. Casciaro, F. Conversano, A. Ragusa, M. A. Malvindi, R. Franchini, A. Greco, T. Pellegrino, and G. Gigli, "Optimal enhancement configuration of silica nanoparticles for ultrasound imaging and automatic detection at conventional diagnostic frequencies," *Invest. Radiol.,* vol. 45, no. 11, pp. 715-724, Nov. 2010.

[19] S. Casciaro, F. Conversano, S. Musio, E. Casciaro, C. Demitri, and A. Sannino, "Full experimental modelling of a liver tissue mimicking phantom for medical ultrasound studies employing different hydrogels," *J. Mater. Sci. Mater. Med.,*vol. 20, no. 4, pp. 983–989, Apr. 2009.

[20] S. Casciaro, C. Demitri, F. Conversano, E. Casciaro, and A. Distante, "Experimental investigation and theoretical modelling of the nonlinear acoustical behaviour of a liver tissue and comparison with a tissue mimicking hydrogel," *J. Mater. Sci. Mater. Med.,* vol. 19, no. 2, pp. 899–906, Feb. 2008.

[21] C. Demitri, A. Sannino, F. Conversano, S. Casciaro, A. Distante, and A. Maffezzoli, "Hydrogel based tissue mimicking phantom for in-vitro ultrasound contrast agents studies," *J. Biomed. Mater. Res. B Appl. Biomater.,* vol. 87B, no. 2, pp. 338-345, Nov. 2008.

[22] R. Greaby, V. Zderic, and S. Vaezy, "Pulsatile flow phantom for ultrasound imageguided HIFU treatment of vascular injuries," *Ultrasound Med. Biol.,*vol. 33, no. 8, pp. 1269–1276, Aug. 2007.

[23] L. Masotti, E. Biagi, M. Scabia, A. Acquafresca, R. Facchini, A. Ricci, and D. Bini, "FEMMINA Real-time, radio-frequency echo-signal equipment for testing novel investigation methods," *IEEE Trans. Ultrason. Ferroelectr. Freq. Control,* vol. 53, no. 10, pp. 1783-1795, Oct. 2006.

[24] A. Bertaccini, A. Franceschelli, R. Schiavina, D. Marchiori, A. Baccos, R. Pernetti, S. Granchi, E. Biagi, I. Masotti, and G. Martorana, "Accuracy of a new echographic method (RULEs, radiofrequency ultrasonic local estimators) in prostate cancer diagnosis," *Anticancer Res.,* vol. 28, no. 3B, pp. 1883-1886, May 2008.

[25] I. Daubechies, "Ten Lectures on Wavelets" (CBMS-NSF Regional Conference Series in Applied Mathematics, vol. 61). Philadelphia, PA, Society for Industrial and Applied Mathematics, 1992.

[26] G. Soloperto, F. Conversano, A. Greco, E. Casciaro, R. Franchini, and S. Casciaro, "Advanced spectral analyses for real-time automatic echographic tissue-typing of simulated tumor masses at different compression stages," *IEEE Trans. Ultrason. Ferroelectr. Freq. Control*, vol. 59, no. 12, pp. 2692-2701, Dec. 2012.

[27] L.G. Delogu, G. Vidili, E. Venturelli, C. Ménard-Moyon, M. A. Zoroddu, G. Pilo, P. Nicolussi, C. Ligios, D. Bedognetti, F. Sgarrella, R. Manetti, and A. Bianco, "Functionalized multiwalled carbon nanotubes as ultrasound contrast agents," *Proc. Natl. Acad. Sci. U S A.,* vol. 109, no. 41, pp. 16612-16617, Oct. 2012.

[28] F. Conversano, A. Greco, E. Casciaro, A. Ragusa, A. Lay-Ekuakille, and S. Casciaro, "Harmonic ultrasound imaging of nanosized contrast agents for multimodal molecular diagnoses," *IEEE Transactions on Instrumentation and Measurement,* vol. 61, no. 12, pp. 1848-1856, Jul. 2012.

[29] M. A. Malvindi, A. Greco, F. Conversano, A. Figuerola, M. Corti, M. Bonora, A. Lascialfari, H. A. Doumari, M. Moscardini, R. Cingolani, G. Gigli, S. Casciaro, T. Pellegrino, and A. Ragusam, "Magnetic/silica nanocomposites as dual-mode contrast agents for combined magnetic resonance imaging and ultrasonography," *Advanced Funct. Mater.,*vol. 21, no. 13, pp. 2548-2555, Jul. 2011.

[30] S. Casciaro, G. Soloperto, A. Greco, E. Casciaro, R. Franchini, F. Conversano, "Effectiveness of functionalized nanosystems for multimodal molecular sensing and imaging in medicine". *IEEE Sensors Journal*, vol. 13, pp.2305-2312, Jun. 2013

[31] G. Soloperto, F. Conversano, A. Greco, E. Casciaro, A. Ragusa, S. Leporatti, A. Lay-Ekuakille, S. Casciaro, "Multiparametric evaluation of the acoustic behaviour of halloysite nanotubes for medical echographic image enhancement". *IEEE Trans. Instrumentation and Measurement* 2014, IN PRESS